INT. J. NUM. METH. HEAT FLUID FLOW, VOL. 3, 121–131 (1993)

FINITE ELEMENT MODELLING OF THE 'NEAR WALL ZONE' OF CONFINED TURBULENT FLOWS: PART II

C. TAYLOR* AND J. Y. XIA†

*Department of Civil Engineering and †Department of Materials Engineering, University College of Swansea, Singleton Park, Swansea SA2 8PP, UK

ABSTRACT

Finite element based solution techniques have been developed to replace the conventional 'wall functions' in the 'near wall zone' of general confined turbulent flows. The technique is validated by application to the turbulent flow and associated heat transfer within a square/rectangular cross-sectioned duct rotating about an axis orthogonal to its longitudinal axis. The predicted results are compared with those from experimental measurements and excellent agreement is obtained when using the advocated methodology.

KEY WORDS Finite element Near wall zone modelling Confined turbulent flows

INTRODUCTION

In a previous publication[1], solution inaccuracies associated with the utilization of logarithmic wall functions were identified and an alternative procedure, replacing such wall functions in the 'near wall zone', was advocated. The 'wall function' approach, derived from Prandtl's mixing length concept, is strictly applicable only when the flow is unidimensional[2]. When two- or three-dimensional flow problems are considered, such a technique, although usually resulting in a converged solution, cannot be considered to be valid. An immediate consequence is the associated inaccuracies in the distribution of turbulent kinetic energy, particularly close to the solid boundary. A cursory examination of the velocity distribution and mass balance, however, is insufficient and a detailed investigation of velocity gradients, turbulence kinetic energy within, and adjacent to, the near wall zone is necessary before inaccuracies can be quantified. These are manifest in both the shear distribution and pressure gradients. In addition, if heat transfer is being quantified, then serious errors can result in the magnitude of local heat flux. This has been adequately demonstrated when numerical 'experiments' were conducted on the prediction of flow and heat transfer in a cooling duct rotating about an axis orthogonal to its longitudinal axis (*Figure 1*). It has been demonstrated that errors, particularly in the prediction of heat transfer, become progressively larger as the rotational speed increases and when the overall flow is less developed.

In the present paper the techniques for depicting the generalized equations of flow near solid boundaries, outlined in Reference 1, are extended to more general flow situations in three dimensions.

GENERALIZED NEAR WALL ZONE SOLUTION PROCEDURE

Techniques[1] developed for the accurate prediction of the distribution of the pertinent variables in the near wall zone were restricted to situations where flows were fully developed. A consequence

0961–5539/93/020121–11$2.00

Received October 1992

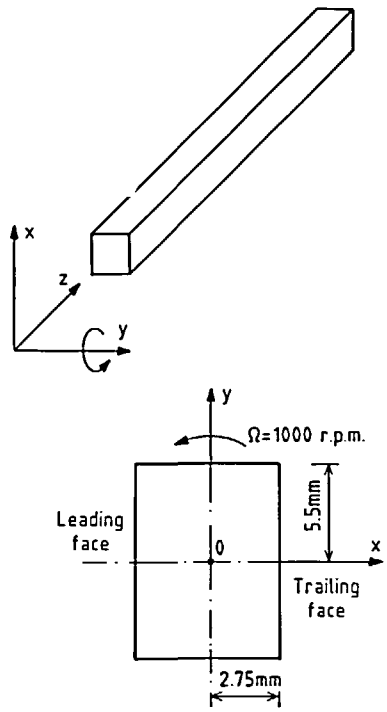

Figure 1 Geometry and co-ordinate system for a rotating rectangular duct

is that resultant velocities were parallel to solid boundaries and invariant with distance along a duct. When such a restriction is imposed then the governing equations could be simplified and unidimensional finite elements normal to the solid boundary could be used to describe the flow field. However, such simplifications are not possible for developing or circulating flows associated with rotating systems or complex geometries. Under these circumstances, the full form of the governing equations have to be utilized and appropriate steps taken to spatially discretize, formulate matrices and develop solution algorithms accordingly.

One technique is to discretize the near wall region using unidimensional elements in each of the global orthogonal directions, x, y and z. The corresponding equations can then be solved for each direction using the corresponding orthogonal finite elements. This leads to an alternate direction implicit solution technique using the following equations:

x-direction:

$$\rho\left[\hat{U}\frac{\partial U}{\partial x}+\hat{V}\frac{\partial \hat{U}}{\partial y}+\hat{W}\frac{\partial \hat{U}}{\partial z}\right]=-\frac{\partial \hat{P}}{\partial x}+\mu_e\left[\frac{\partial^2 U}{\partial x^2}+\frac{\partial^2 \hat{U}}{\partial y^2}+\frac{\partial^2 \hat{U}}{\partial z^2}\right]+X \tag{1}$$

y-direction:

$$\rho\left[\hat{U}\frac{\partial \hat{V}}{\partial x}+\hat{V}\frac{\partial V}{\partial y}+\hat{W}\frac{\partial \hat{V}}{\partial z}\right]=-\frac{\partial \hat{P}}{\partial y}+\mu_e\left[\frac{\partial^2 \hat{V}}{\partial x^2}+\frac{\partial^2 V}{\partial y^2}+\frac{\partial^2 \hat{V}}{\partial z^2}\right]+Y \tag{2}$$

z-direction:

$$\rho\left[\hat{U}\frac{\partial \hat{W}}{\partial x}+\hat{V}\frac{\partial \hat{W}}{\partial y}+\hat{W}\frac{\partial W}{\partial z}\right]=-\frac{\partial \hat{P}}{\partial z}+\mu_e\left[\frac{\partial^2 \hat{W}}{\partial x^2}+\frac{\partial^2 \hat{W}}{\partial y^2}+\frac{\partial^2 W}{\partial z^2}\right]+Z \tag{3}$$

where ρ is the fluid density, U, V, W the time-averaged velocities in the x, y, z orthogonal global

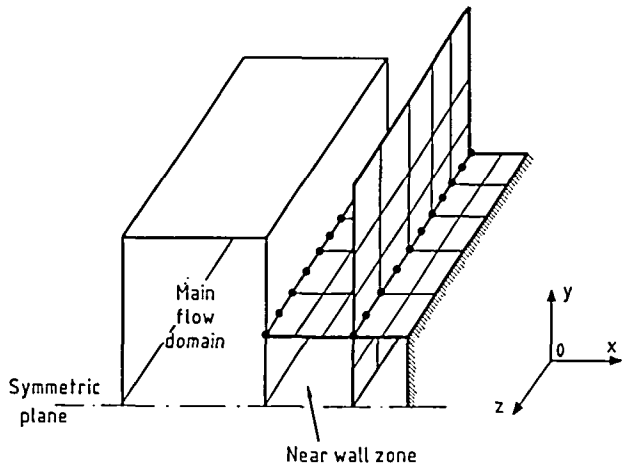

Figure 2 Two typical sets of 2-D near wall elements

directions, respectively, μ_e the effective velocity, i.e. $(\mu + \mu_t)$, μ_t the turbulent viscosity and X, Y, Z are the body forces again in the x, y, z directions, respectively. The overcaret can denote values derived by solving corresponding equations in directions other than that applicable to the equation being analysed. Additionally, for variables being currently analysed, the overcaret denotes previous iteration values on that variable which linearizes, with respect to that variable, the equation being analysed.

A segregated approach is used such that $\hat{P}$ is derived from a pressure Poisson equation. Details of the segregation procedure can be found in Reference 3. Each equation is solved in the appropriate direction and an alternative direction implicit procedure adopted. As indicated previously, the pressure term, at each iteration, is recovered using a segregated approach[4]. Although the method is relatively simple, the rate of convergence can be affected, to a considerable degree, by the choice of initial conditions. This is in common with most iterative procedures where the majority of terms in the current equation being solved are previous iteration values from alternate directions. However, the solver proved to be quite successful[4] when analysing two-dimensional turbulent flows.

If variations in the independent variables parallel to a solid boundary in the x, y plane (*Figure 2*) are small then unidimensional or two-dimensional elements arranged in the x–z and y–z planes can be used. When conducting analyses using such element configurations, with the more stringent spatial integration, converged solutions are obtained, as expected, more rapidly than with unidimensional elements in three directions. However, this is offset by substantial increases in both computer storage requirements and CPU time.

In general, a better choice of element configuration, which also accommodates variable variations in both directions in the transverse x–y plane, is that shown on *Figure 3*. In this case two-dimensional elements are used in the transverse plane which, in the near wall zone, are connected by one-dimensional elements in the axial, z, direction. This system ensured rapid convergence and avoids, for developing or convective flows, the greater computational demands commensurate with full spatial discretization. Under these conditions the governing equations are:

x-direction:

$$\rho\left[\hat{U}\frac{\partial U}{\partial x} + \hat{V}\frac{\partial U}{\partial y} + \hat{W}\frac{\partial \hat{U}}{\partial z}\right] = -\frac{\partial \hat{P}}{\partial x} + \mu_e\left[\frac{\partial^2 U}{\partial x^2} + \frac{\partial^2 U}{\partial y^2} + \frac{\partial^2 \hat{U}}{\partial z^2}\right] + X \tag{4}$$

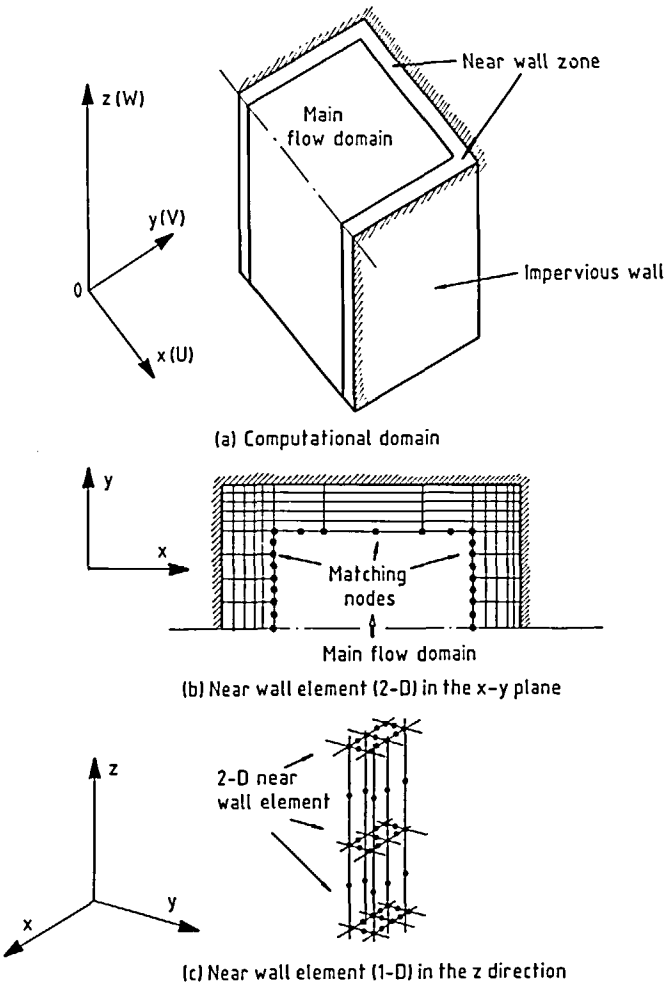

Figure 3 Diagram illustrating matching of the main flow domain with two-dimensional elements/uni-dimensional elements

y-direction:

$$\rho\left[\hat{U}\frac{\partial V}{\partial x}+\hat{V}\frac{\partial V}{\partial y}+\hat{W}\frac{\partial \hat{V}}{\partial z}\right]=-\frac{\partial \hat{P}}{\partial y}+\mu_e\left[\frac{\partial^2 V}{\partial x^2}+\frac{\partial^2 V}{\partial y^2}+\frac{\partial^2 \hat{V}}{\partial z^2}\right]+Y \tag{5}$$

z-direction:

$$\rho\left[\hat{U}\frac{\partial W}{\partial x}+\hat{V}\frac{\partial W}{\partial y}+\hat{W}\frac{\partial \hat{W}}{\partial z}\right]=-\frac{\partial \hat{P}}{\partial z}+\mu_e\left[\frac{\partial^2 W}{\partial x^2}+\frac{\partial^2 W}{\partial y^2}+\frac{\partial^2 \hat{W}}{\partial z^2}\right]+Z \tag{6}$$

Using the segregated method[3] the pressure is recovered from the Poisson equation:

$$\frac{\partial^2 P}{\partial x^2}+\frac{\partial^2 P}{\partial y^2}+\frac{\partial^2 \hat{P}}{\partial z^2}=2\rho(\hat{J}+\hat{D}^2) \tag{7}$$

where

$$J = \begin{bmatrix} \frac{\partial U}{\partial x} & \frac{\partial V}{\partial x} & \frac{\partial W}{\partial x} \\ \frac{\partial U}{\partial y} & \frac{\partial V}{\partial y} & \frac{\partial W}{\partial y} \\ \frac{\partial U}{\partial z} & \frac{\partial V}{\partial z} & \frac{\partial W}{\partial z} \end{bmatrix}$$

and

$$D = \frac{\partial U}{\partial x} + \frac{\partial V}{\partial y} + \frac{\partial W}{\partial z}$$

For the one equation model of turbulence the necessary closure equation on the turbulent kinetic energy, k, is

$$\rho\left(\hat{U}\frac{\partial k}{\partial x} + \hat{V}\frac{\partial k}{\partial y} + \hat{W}\frac{\partial k}{\partial z}\right) = \left(\mu + \frac{\mu_t}{\sigma_k}\right)\left(\frac{\partial^2 k}{\partial x^2} + \frac{\partial^2 k}{\partial y^2} + \frac{\partial^2 k}{\partial z^2}\right) - C_D\rho\frac{k^{3/2}}{l} - \mu_e C_k \tag{8}$$

in which C_D is a constant, l a local length scale and G_k is given by:

$$G_k = 2\left[\left(\frac{\partial U}{\partial x}\right)^2 + \left(\frac{\partial V}{\partial y}\right)^2 + \left(\frac{\partial W}{\partial z}\right)^2\right] + \left(\frac{\partial U}{\partial y} + \frac{\partial V}{\partial x}\right)^2 + \left(\frac{\partial U}{\partial z} + \frac{\partial W}{\partial x}\right)^2 + \left(\frac{\partial V}{\partial z} + \frac{\partial W}{\partial y}\right)^2$$

BOUNDARY CONDITIONS AND 'NEAR WALL' MATCHING

In the transverse, x–y, plane, when incorporating two-dimensional elements in the near wall zone, boundary conditions are required at both the solid boundary and at the interface between the main flow domain and the near wall zone (*Figure 4*).

Solid wall

At all points on the solid wall the 'no-slip' condition is satisfied. Since no turbulence exists and no flow normal to the wall, then both the turbulence kinetic energy, k, and the pressure gradient $\partial P/\partial n$ are zero. Therefore,

$$\left.\begin{matrix} U \\ V \\ W \\ k \\ \frac{\partial P}{\partial n} \end{matrix}\right\} = 0$$

where n denotes the direction of the outward normal to the boundary.

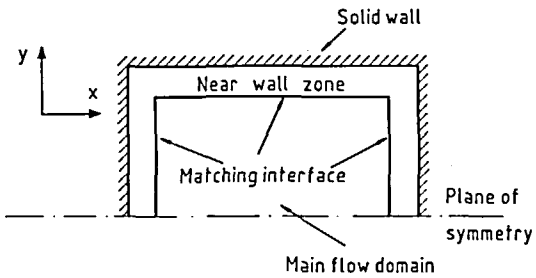

Figure 4 Near wall zone boundary

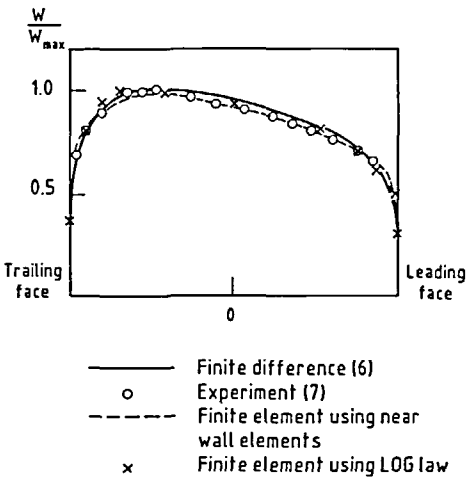

Figure 5 Comparison of axial velocity profiles along the plane of symmetry ($Ro = 0.01$)

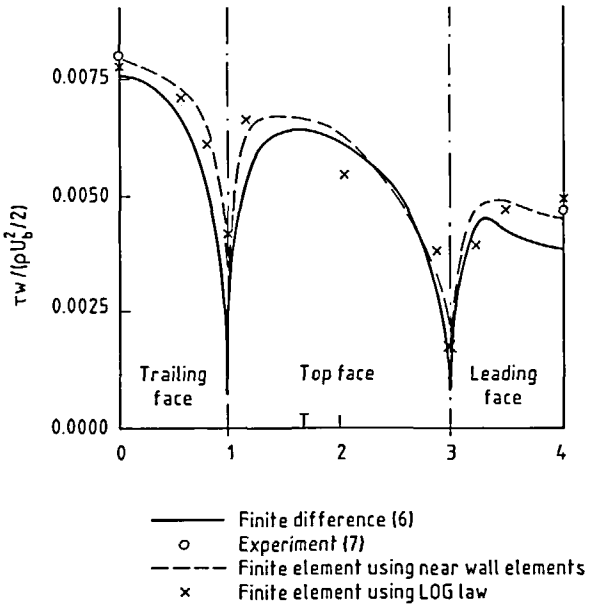

Figure 6 Comparison of local wall shear stress along the wall surface ($Ro = 0.01$)

Plane of symmetry

All gradients normal to this plane can be set to zero such that:

$$\left.\begin{matrix}\dfrac{\partial U}{\partial y}\\[2ex] \dfrac{\partial V}{\partial y}\\[2ex] \dfrac{\partial W}{\partial y}\end{matrix}\right\} = 0, \qquad \frac{\partial k}{\partial y} = \frac{\partial P}{\partial y} = 0$$

Interfacial conditions

In order to initiate a numerically based solution procedure for the Navier–Stokes equations including any closure equations, an initial distribution of variables must be assumed to start an iterative process.

In common with the flow domain interfacial boundary conditions are required at the limit of the near wall zone. The iterative procedure adopted is as follows: (i) set boundary conditions;

(ii) set an initial distribution of all variables both in the main flow domain and the near wall zone; (iii) solve the governing equation in the main flow domain to obtain U, V, W, P and k, details of this procedure can be found in Reference 1; (iv) using element shape functions, evaluate the normal gradients of all variables along the interface; (v) impose the values obtained in (iv) at the interface and solve, for the axial gradients of all the variables in the near wall zone. Using (4) to (8), solve, using an alternate direction implicit iterative procedure, for all variables in the near wall zone; (vi) values of the primitive variables and kinetic energy obtained in (v) are then imposed on the interface, as boundary conditions for the main flow domain; (vii) repeat (iii) to (vi) to convergence.

EXAMPLES AND DISCUSSION

Fully developed flow is amongst the type of problems previously analysed using unidimensional elements in the near wall zone[1]. An example of current interest is that of fully developed flow in a rotating square duct of prismoidal section, 2.75 mm square, rotating about an axis orthogonal to its longitudinal axis. The Rossby number is 0.01 and is calculated from: $Ro = \Omega d/U_b$ in which Ω is the angular speed of rotation, d the hydraulic diameter of the duct and U_b the bulk longitudinal velocity.

For this problem the algebraic stress turbulence model[5] was found to be the more accurate and the longitudinal velocity profile obtained is compared with both finite difference predictions[6] and experimental measurements[7], as shown in *Figure 5*. Solutions obtained when universal laws and element discretization are used in the near wall zone are also presented. The corresponding distribution of wall shear stress around the inside face of the duct is shown on *Figure 6*.

The results indicate that, due to Coriolis effects arising from the duct rotation, forces the high momentum fluid towards the trailing face resulting in a lower wall shear on the leading face. The corner stagnation conditions correspond to the near zero shear as illustrated on *Figure 6*. It is immediately apparent that, although differences in the longitudinal velocity profile are small, there are significant differences in the shear stresses as obtained from the different techniques. Both the finite difference method[6] and logarithmic law seem to be generally under-predictive. The better agreement between experiment and theory is when finite elements are used in the near wall zone. Scrutiny of the longitudinal velocity profiles and conservation of mass is, therefore, not conclusive and, to this point, a clear investigation should be undertaken by comparing wall shear stresses. Evidently, this depends on local velocity gradients which are primarily dependent on the spatial description of variables near the solid wall.

Having illustrated that the near wall element technique could be superior to the other methods, a more stringent example will now be considered. In this case developing flow is considered with rotation and heat transfer.

In this example, the same Rossby number, but associated with a rectangular rotating duct of dimensions indicated on *Figure 1*, is considered. Upstream boundary conditions, for the flow only, consist of a constant uniform longitudinal velocity, top hat, and zero secondary flow. It is apparent, from *Figure 7*, that secondary patterns are generated, as expected, immediately downstream of the entrance. These gradually develop into a single secondary pattern at progressive downstream sections. The discrepancies between the case where log laws are used and when elements are employed are significant near the entry but gradually diminish with longitudinal distance. This is to be expected since the universal profile can, in reality, only accommodate unidimensional flow and, therefore, cannot be considered to be accurate, particularly at the upstream sections.

In this case the duct was subjected to a heat flux. The coupled solid/fluid computational method[8] was adopted and the boundary conditions are illustrated as in *Figure 8*. The resulting temperature contours are as shown in *Figure 9*. Although these show differences between both

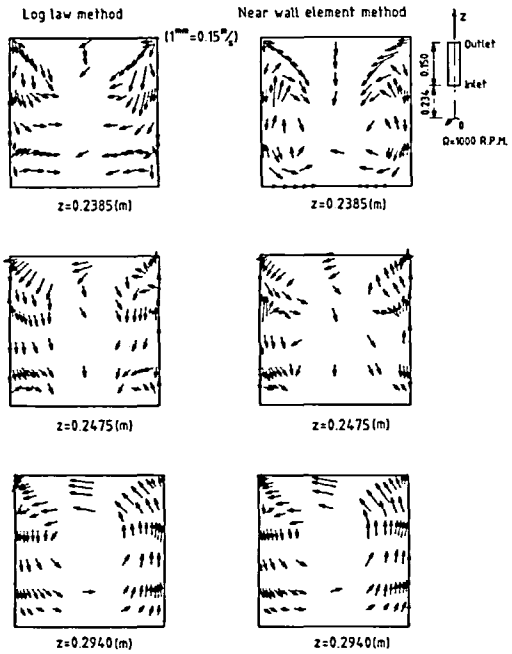

Figure 7 Comparison of secondary velocity pattern in a rotating rectangular duct (developing flow, $Ro = 0.01$)

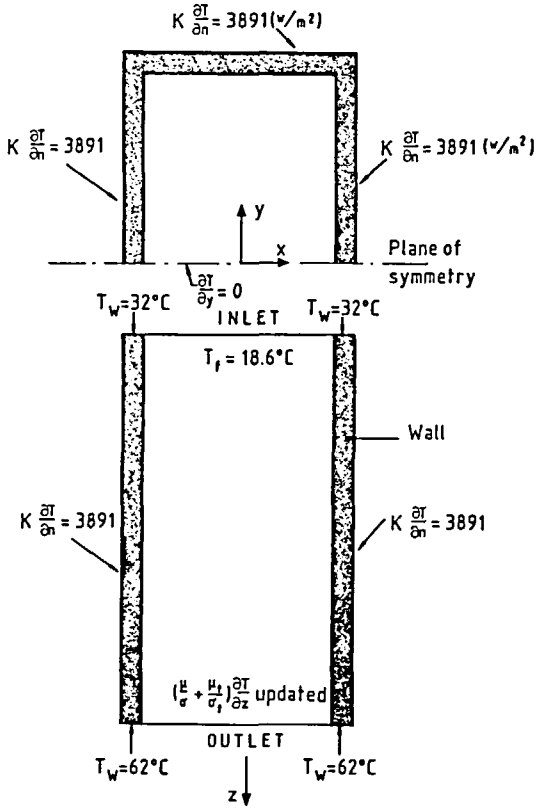

Figure 8 Boundary conditions for coupled solid/fluid heat transfer system in a rotating rectangular duct

Table 1 Comparison of heat transfer in a rectangular rotating duct using different near wall modelling (developing flow $Ro = 0.010$)

Axial position, z (cm)		23.625	23.850	24.300	24.750	25.575	26.400	27.900	29.400	31.650	33.900	36.150
Tempera-	Log law	32.32	35.11	40.41	45.36	53.54	60.64	71.11	78.85	84.89	83.23	73.59
ture,	N.W.E	32.17	34.81	39.85	44.54	52.33	59.09	69.07	76.52	82.56	81.53	72.75
T(°C)	Experiments	32.15	34.50	39.60	44.44	52.30	59.10	68.90	72.01	75.34	77.03	72.89
Nusselt	Log law		95.17		52.34		33.67		24.56		24.31	
number	N.W.E.		118.91		55.37		34.89		25.55		25.51	
	Experiments		130.0		60.00		37.00		28.50		29.70	

models, a more informative comparison, relating to Nusselt numbers, is given on *Table 1*. For present purposes the Nusselt number is defined as follows:

$$Nu = \frac{fd}{K\Delta T_w}$$

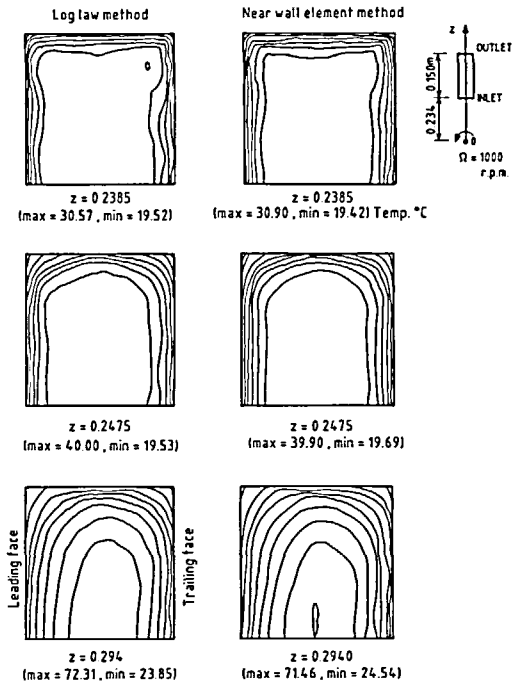

Figure 9 Comparison of temperature contours in a rotating rectangular duct (developing flow)

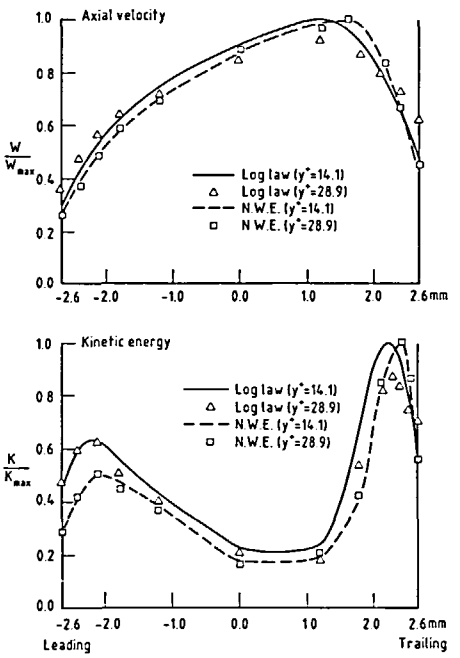

Figure 10 Comparison of axial velocity profiles and turbulent kinetic energy profiles in a rotating square duct ($Ro = 0.075$) using an ASM model (developed flow)

in which f is the local heat flux at the solid boundary and ΔT_w the difference in temperature between the solid wall and the local bulk value.

Again, although the temperature plots do not show any significant differences, the differences between Nusselt numbers is quite appreciable, being of the order of 25% at the upstream sections. Since the values associated with the near wall element methodology are consistently larger, the recirculation must be correspondingly greater. This tends to draw more heat from the solid surfaces into the fluid. Again the values determined using the near wall element technique are significantly closer to the experimental results with a maximum error of approximately 12%.

Having established that the near wall element technique results are consistently closer to experiment, attention is turned to flows with a higher Rossby number and a limited parametric study into the effect of varying the location of the interface between the main flow domain and the near wall zone. The square duct is that defined previously and the Rossby number has been increased to 0.075. The resulting distributions of axial velocity and turbulence kinetic energy at the plane of symmetry for different locations of the interface are shown in *Figure 10*. These plots illustrate a marked difference between the profiles obtained under different conditions. It is clear that there are also significant differences between the results obtained when using universal profiles at different y^+ magnitudes. However, such discrepancies are not apparent when near wall elements are used. A similar conclusion can be drawn from a scrutiny of the turbulence kinetic energy profiles. Indeed, in this case the maximum difference between the worst log law case and the near wall element results is approximately 30%. A most disconcerting feature of this exercise is the large variation in the results when using the log law technique and simply varying the y^+ magnitudes. It should be pointed out at this juncture that the y^+ values used are within those advocated to be acceptable by most other numerical analysts. This is obviously open to question.

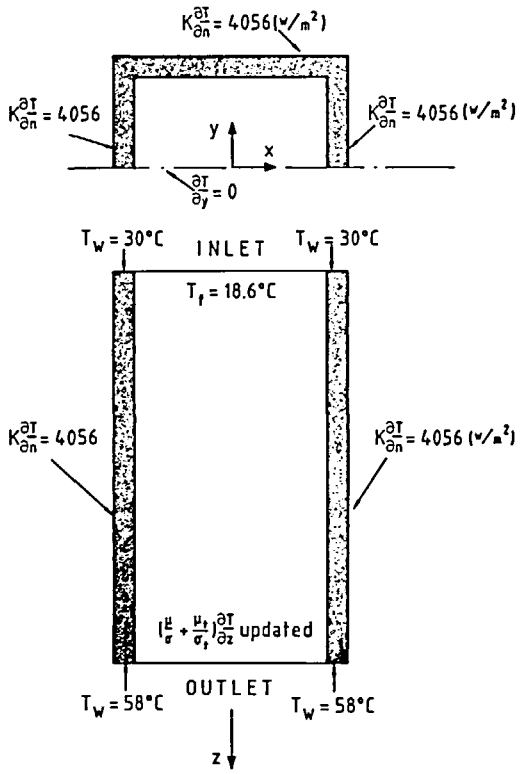

Figure 11 Boundary conditions for coupled solid/fluid heat transfer system in a rotating square duct

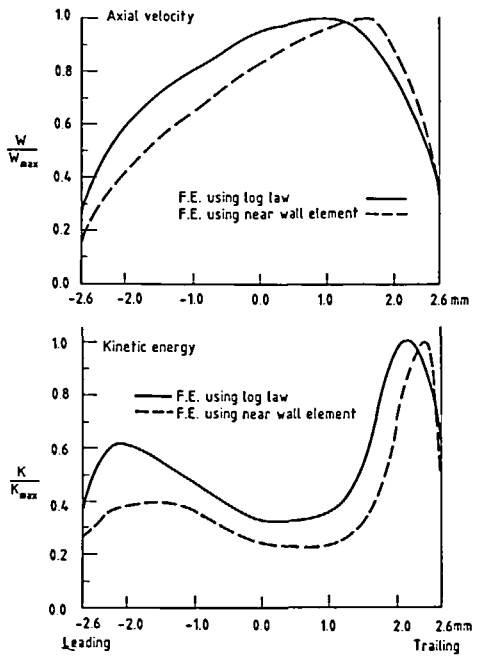

Figure 12 Comparisons of axial velocity profiles and turbulent kinetic energy profiles in a rotating square duct ($Ro = 0.075$) using ASM model (developing flow at a section 1/4 length from outlet)

For developing flow, in the same duct with Rossby number and thermal conditions, illustrated on *Figure 11*, the differences between the axial velocities and kinetic energies, again at the plane of symmetry, are more pronounced (*Figure 12*). A more distorted pattern is obtained when using the near wall elements such that the higher momentum fluid moves towards the trailing face.

The significance of the variation in the longitudinal velocity is again reflected in the variation of wall shear stress. This is not presented but the trend is similar to that reproduced in *Figure 6*.

Comparing heat transfer characteristics there are significant differences between the calculated values, particularly Nusselt number (*Table 2*). Once again, the discrepancies are larger near the duct inlet, being of the order of 25% although maximum temperature differences are only 6%.

CONCLUSIONS

An alternative technique is suggested and tested for the numerical evaluation of independent variables within the near wall zone of confined turbulent flow. The advocated method utilizes conventional finite element discretization in the region close to the wall which captures the characteristics of the flow in all directions. This has been shown to be superior to the usually advocated 'universal laws' which not only misrepresents the flow pattern but is also very restricted with regard to the location of the limit of the near wall zones. This is not the case when finite elements are used.

The apparent independence of the results on the location of the near wall zone is a distinct

Table 2 Comparison of heat transfer in a square rotating duct using different near wall modelling (developing flow, $Ro = 0.075$)

Axial position, z (cm)		23.625	23.850	24.300	24.750	25.575	26.400	27.900	29.400	31.650	33.900	36.150
Tempera-	Log law	30.23	32.94	38.08	42.86	50.70	57.45	67.17	74.09	79.49	78.56	69.98
ture, T(°C)	N.W.E.	30.06	32.41	37.03	41.63	48.93	55.14	64.04	70.62	76.12	75.73	67.91
Nusselt	Log law		135.7		81.3		40.1		34.5		34.2	
number	N.W.E.		178.8		89.5		44.7		37.8		37.4	

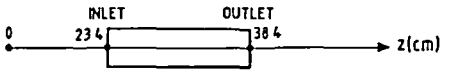

advantage when undertaking an analysis. In reality this value must be checked, particularly when log laws are employed, to ensure that y^+ remains within a very narrow band and even for the small band tested herein the variations can be significant.

Consequent to the inability of log laws to predict the flow field is the marked effect on the recirculation pattern and heat transfer. Although a cursory inspection of longitudinal profiles could lead to the acceptance of predictions, a much closer scrutiny in terms of shear stress and, if applicable, heat transfer should always be undertaken.

ACKNOWLEDGEMENTS

The authors wish to acknowledge the financial support of Rolls Royce plc (Bristol) and collaboration with Professor W.D. Morris of the Department of Mechanical Engineering at the University of Swansea.

REFERENCES

1 Xia, J.Y., Taylor, C. and Medwell, J.O. Finite element modelling of near wall zone of confined turbulent flows, *Eng. Comput.* 6, 127–132 (1989)
2 Davies, J.T. *Turbulence Phenomena*, Academic Press, New York (1972)
3 Schneider, G.E., Raithby, G.D. and Kovanovich, M.M. Finite element analysis of incompressible fluid flow incorporating equal order pressure and velocity interpolation, *Proc. First Int. Conf. Num. Meth. Laminar Turbulent Flow* (Eds C. Taylor *et al.*) Pentech Press, London (1978)
4 Gheissary, A.A. Some limitation of turbulence modelling and the development of techniques for mapping the near-wall zones, *PhD Thesis*, University College of Swansea (1988)
5 Xia, J.Y., Taylor, C. and Medwell, J.O. Finite element modelling of turbulent secondary motion in ducts of square cross-section, *Flow Modelling in Industrial Processes*, Ellis Horwood, Chichester (1989)
6 Jacovides, H. and Launder, B.E. Turbulent momentum and heat transport in square-sectioned ducts rotating in orthogonal mode, *Interim Report, UMIST, TFD/86/* (1986)
7 Launder, B.E. The effect of Coriolis force on fully developed flow in a rotating duct, Unpublished Report, MIT Gas Turbine Laboratory (1965)
8 Medwell, J.O., Morris, W.D., Xia, J.Y. and Taylor, C. An investigation of convective heat transfer in a rotating coolant channel, *J. Turbomach.* 113, 354–359 (1991)